

03.01.2008, Spåtind, Norway

Single production of doubly charged Higgsinos at linear $e^- e^-$ colliders

Santosh Kumar Rai

Helsinki Institute of Physics

Finland

work done with:
arXiv:0710.2415

M. Frank & K. Huitu
(To appear in Phys. Rev. D)

Outline

- ★ *Left-Right Supersymmetry*
- ★ *Higgs Sector and Doubly Charged States*
- ★ *Production of doubly charged Higgsinos*
- ★ *Results*
- ★ *Conclusions & Outlook*

Left-Right Supersymmetry

- ★ *Supersymmetry is by far the most popular option for beyond standard model physics.*
- ★ *Neutrino mass generation in its minimal version*
R-parity violation
Right-handed neutrinos (seesaw)
- ★ *Supersymmetric grand unified theories with left-right symmetry can explain neutrino masses without requiring the added conditions.*

Left-Right Supersymmetry

- ★ *Supersymmetric left-right theories (LRSUSY) are based on the product group:*

$$SU(3)_C \times SU(2)_L \times SU(2)_R \times U(1)_{B-L}$$

- ★ *This product group is broken to $SU(3)_C \times U(1)_{em}$ by giving vevs to fields in the Higgs sector.*

$$SU(2)_R \times U(1)_{B-L} \longrightarrow U(1)_Y$$

- ★ *Neutrino masses are induced by the see-saw mechanism through introduction of Higgs triplet fields.*

Higgs sector

- ★ *The left-right symmetry is broken at a scale $\langle \Delta_R^0 \rangle = v_R$*
- ★ *The bi-doublet Higgs fields break the $SU(2)_L \times U(1)_Y$*
- ★ *Supersymmetry requires other Higgs multiplets to cancel chiral anomalies among the fermionic partners*

$$\begin{aligned}
 \Phi_1 &= \begin{pmatrix} \Phi_{11}^0 & \Phi_{11}^+ \\ \Phi_{12}^- & \Phi_{12}^0 \end{pmatrix} \sim (1, 2, 2, 0), & \Phi_2 &= \begin{pmatrix} \Phi_{21}^0 & \Phi_{21}^+ \\ \Phi_{22}^- & \Phi_{22}^0 \end{pmatrix} \sim (1, 2, 2, 0) \\
 \Delta_L &= \begin{pmatrix} \frac{1}{\sqrt{2}}\Delta_L^- & \Delta_L^0 \\ \Delta_L^{--} & -\frac{1}{\sqrt{2}}\Delta_L^- \end{pmatrix} \sim (1, 3, 1, -2), & \delta_L &= \begin{pmatrix} \frac{1}{\sqrt{2}}\delta_L^+ & \delta_L^{++} \\ \delta_L^0 & -\frac{1}{\sqrt{2}}\delta_L^+ \end{pmatrix} \sim (1, 3, 1, 2), \\
 \Delta_R &= \begin{pmatrix} \frac{1}{\sqrt{2}}\Delta_R^- & \Delta_R^0 \\ \Delta_R^{--} & -\frac{1}{\sqrt{2}}\Delta_R^- \end{pmatrix} \sim (1, 1, 3, -2), & \delta_R &= \begin{pmatrix} \frac{1}{\sqrt{2}}\delta_R^+ & \delta_R^{++} \\ \delta_R^0 & -\frac{1}{\sqrt{2}}\delta_R^+ \end{pmatrix} \sim (1, 1, 3, 2)
 \end{aligned}$$

$$Q = \begin{pmatrix} u \\ d \end{pmatrix} \sim \left(3, 2, 1, \frac{1}{3}\right), \quad Q^c = \begin{pmatrix} d^c \\ u^c \end{pmatrix} \sim \left(3^*, 1, 2, -\frac{1}{3}\right),$$

★ The matter fields:

$$L = \begin{pmatrix} \nu \\ e \end{pmatrix} \sim (1, 2, 1, -1), \quad L^c = \begin{pmatrix} e^c \\ \nu^c \end{pmatrix} \sim (1, 1, 2, 1),$$

★ *The most general superpotential one can write is*

$$W = \mathbf{Y}_Q^{(i)} Q^T \Phi_i i\tau_2 Q^c + \mathbf{Y}_L^{(i)} L^T \Phi_i i\tau_2 L^c + i(\mathbf{h}_U L^T \tau_2 \delta_L L + \mathbf{h}_U L^{cT} \tau_2 \Delta_R L^c) \\ + \mu_3 [Tr(\Delta_L \delta_L + \Delta_R \delta_R)] + \mu_{ij} Tr(i\tau_2 \Phi_i^T i\tau_2 \Phi_j) + W_{NR}$$

and the soft terms as

$$\mathcal{L}_{soft} = [\mathbf{A}_Q^i \mathbf{Y}_Q^{(i)} \tilde{Q}^T \Phi_i i\tau_2 \tilde{Q}^c + \mathbf{A}_L^i \mathbf{Y}_L^{(i)} \tilde{L}^T \Phi_i i\tau_2 \tilde{L}^c + i\mathbf{A}_{LR} \mathbf{h}_U (\tilde{L}^T \tau_2 \delta_L \tilde{L} + \tilde{L}^{cT} \tau_2 \Delta_R \tilde{L}^c) \\ + m_\Phi^{(ij)2} \Phi_i^\dagger \Phi_j] + [(m_L^2)_{ij} \tilde{l}_{Li}^\dagger \tilde{l}_{Lj} + (m_R^2)_{ij} \tilde{l}_{Ri}^\dagger \tilde{l}_{Rj}] - M_{LR}^2 [Tr(\Delta_R \delta_R) + Tr(\Delta_L \delta_L) + h.c.] \\ - [B\mu_{ij} \Phi_i \Phi_j + h.c.]$$

- ★ *The vevs to the different scalar multiplets contributing to the symmetry breaking down to $U(1)_{em}$*

$$\langle \Phi_1 \rangle = \begin{pmatrix} \kappa_1 & 0 \\ 0 & \kappa'_1 e^{i\omega_1} \end{pmatrix}, \quad \langle \Phi_2 \rangle = \begin{pmatrix} \kappa'_2 e^{i\omega_2} & 0 \\ 0 & \kappa_2 \end{pmatrix}, \quad \langle \Delta_L \rangle = \begin{pmatrix} 0 & v_{\Delta_L} \\ 0 & 0 \end{pmatrix},$$

$$\langle \delta_L \rangle = \begin{pmatrix} 0 & 0 \\ v_{\delta_L} & 0 \end{pmatrix}, \quad \langle \Delta_R \rangle = \begin{pmatrix} 0 & v_{\Delta_R} \\ 0 & 0 \end{pmatrix}, \quad \langle \delta_R \rangle = \begin{pmatrix} 0 & 0 \\ v_{\delta_R} & 0 \end{pmatrix}.$$

- ★ *Due to the extended Higgs sector, the spectrum has additional higgsinos, both neutral, singly charged and doubly charged.*

$$\Delta_L^{++}, \Delta_R^{++}, \delta_L^{++}, \delta_R^{++}$$

Mass term:

$$\mathcal{L}_{\tilde{\Delta}} = -M_{\tilde{\Delta}^{--}} \tilde{\Delta}_L^{--} \tilde{\delta}_L^{++} - M_{\tilde{\Delta}^{--}} \tilde{\Delta}_R^{--} \tilde{\delta}_R^{++} + h.c.,$$

where

$$M_{\tilde{\Delta}^{--}} = \mu_3.$$

Representative points

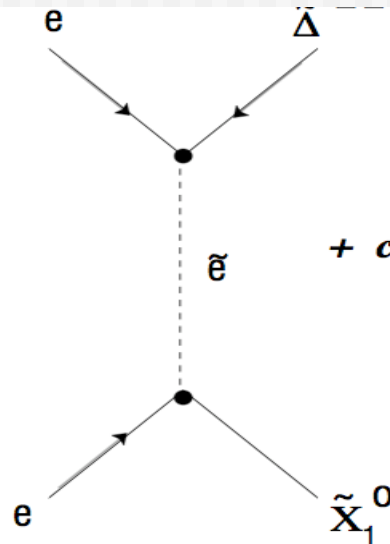
<p>Sample point A :</p> <p>$\tan \beta = 20$</p> <p>$M_{B-L} = 25 \text{ GeV}$</p> <p>$\mu_1 = 1000 \text{ GeV}$</p> <p>$v_{\Delta_L} = 1.5 \times 10^{-8} \text{ GeV}$</p> <p>$v_{\Delta_R} = 3000 \text{ GeV}$</p>	<p>$M_L = M_R = 250 \text{ GeV}$</p> <p>$\mu_3 = 300 \text{ GeV}$</p> <p>$v_{\delta_L} = 1.0 \times 10^{-8} \text{ GeV}$</p> <p>$v_{\delta_R} = 1000 \text{ GeV}$</p>	<p>$M_{\tilde{\chi}_1^0} = 91.8 \text{ GeV}$</p> <p>$M_{\tilde{\chi}_3^0} = 250.0 \text{ GeV}$</p> <p>$M_{\tilde{\chi}_1^\pm} = 249.0 \text{ GeV}$</p> <p>$M_{\tilde{\chi}_3^\pm} = 911.7 \text{ GeV}$</p>	<p>$M_{\tilde{\chi}_2^0} = 180.6 \text{ GeV}$</p> <p>$M_{\tilde{\chi}_2^\pm} = 300.0 \text{ GeV}$</p>
<p>Sample point B :</p> <p>$\tan \beta = 30$</p> <p>$M_{B-L} = 100 \text{ GeV}$</p> <p>$\mu_1 = 500 \text{ GeV}$</p> <p>$v_{\Delta_L} = 1.5 \times 10^{-8} \text{ GeV}$</p> <p>$v_{\Delta_R} = 2500 \text{ GeV}$</p>	<p>$M_L = M_R = 500 \text{ GeV}$</p> <p>$\mu_3 = 500 \text{ GeV}$</p> <p>$v_{\delta_L} = 1.0 \times 10^{-8} \text{ GeV}$</p> <p>$v_{\delta_R} = 1500 \text{ GeV}$</p>	<p>$M_{\tilde{\chi}_1^0} = 217.3 \text{ GeV}$</p> <p>$M_{\tilde{\chi}_3^0} = 450.0 \text{ GeV}$</p> <p>$M_{\tilde{\chi}_1^\pm} = 447.8 \text{ GeV}$</p> <p>$M_{\tilde{\chi}_3^\pm} = 500 \text{ GeV}$</p>	<p>$M_{\tilde{\chi}_2^0} = 441.7 \text{ GeV}$</p> <p>$M_{\tilde{\chi}_2^\pm} = 500.0 \text{ GeV}$</p>

Table 1: Sample points of the particle spectrum. The left column contains the input values for the parameters of the model, while the right column lists the masses of the lightest the neutralinos and charginos corresponding to the choice of input parameters.

Single production mode at linear $e^- e^-$ colliders

$$e^- e^- \longrightarrow \tilde{\Delta}^{--} \tilde{\chi}_1^0$$

ideal for production of such doubly charged exotics



allows to probe a large range of masses of the doubly charged Higgsinos

relevant couplings

$$\tilde{\Delta}_R^{--} \tilde{l}_R^- \tilde{l}_R^- \quad - 2h_u C^{-1} P_R$$

$$\tilde{\Delta}_L^{--} \tilde{l}_L^- \tilde{l}_L^- \quad - 2h_u C^{-1} P_L$$

$$\ell^- \tilde{\ell}_L^- \chi_k^0 \quad \rightarrow \quad \frac{1}{\sqrt{2}} (g_L N_{k1} + g_V N_{k3}) P_L$$

$$\ell^- \tilde{\ell}_R^- \chi_k^0 \quad \rightarrow \quad \frac{1}{\sqrt{2}} (g_R N_{k2}^* + g_V N_{k3}^*) P_R$$

Bounds on the Yukawa couplings

$$h_{e\mu}h_{ee} < 3.2 \times 10^{-11} \text{ GeV}^{-2} \cdot M_{\Delta^{--}}^2 \quad \text{from } \mu \rightarrow \bar{e}ee,$$

$$h_{e\mu}h_{\mu\mu} < 2 \times 10^{-10} \text{ GeV}^{-2} \cdot M_{\Delta^{--}}^2 \quad \text{from } \mu \rightarrow e\gamma,$$

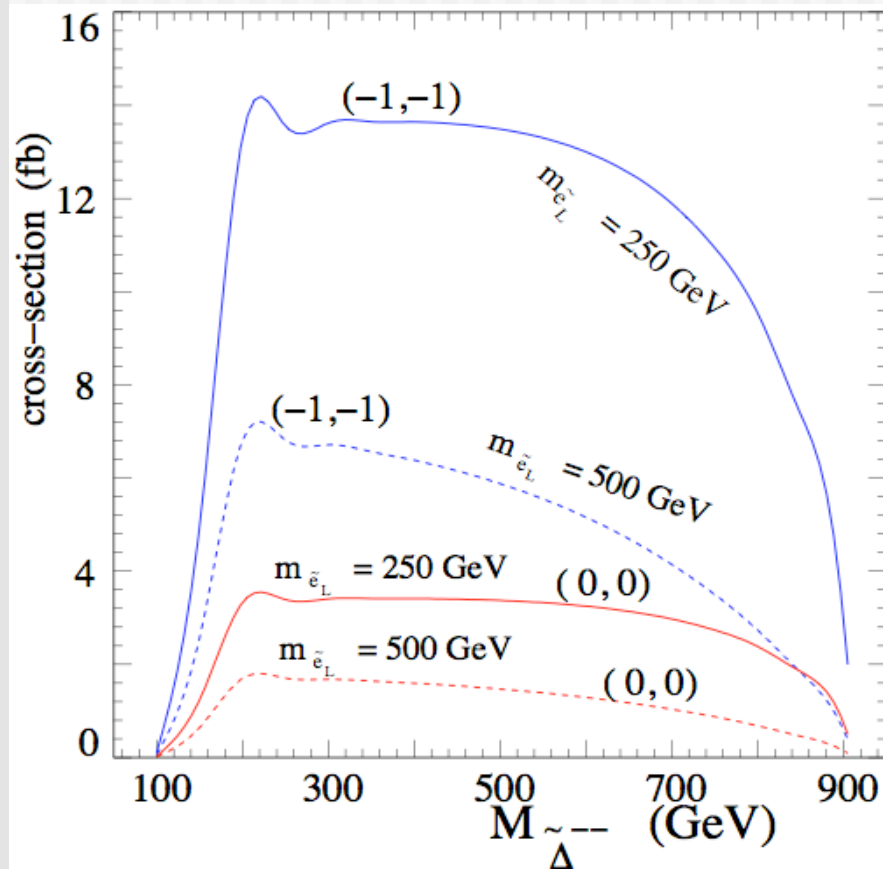
$$h_{ee}^2 < 9.7 \times 10^{-6} \text{ GeV}^{-2} \cdot M_{\Delta^{--}}^2 \quad \text{from Bhabha scattering,}$$

$$h_{\mu\mu}^2 < 2.5 \times 10^{-5} \text{ GeV}^{-2} \cdot M_{\Delta^{--}}^2 \quad \text{from } (g-2)_{\mu},$$

$$h_{ee}h_{\mu\mu} < 2.0 \times 10^{-7} \text{ GeV}^{-2} \cdot M_{\Delta^{--}}^2 \quad \text{from muonium – antimuonium transition.}$$

We choose $\mathbf{h}_{II} = 0.1$ which is consistent with the bounds.
Larger values allowed with a large mass for Δ^{--}

Production cross-section of the left-chiral states



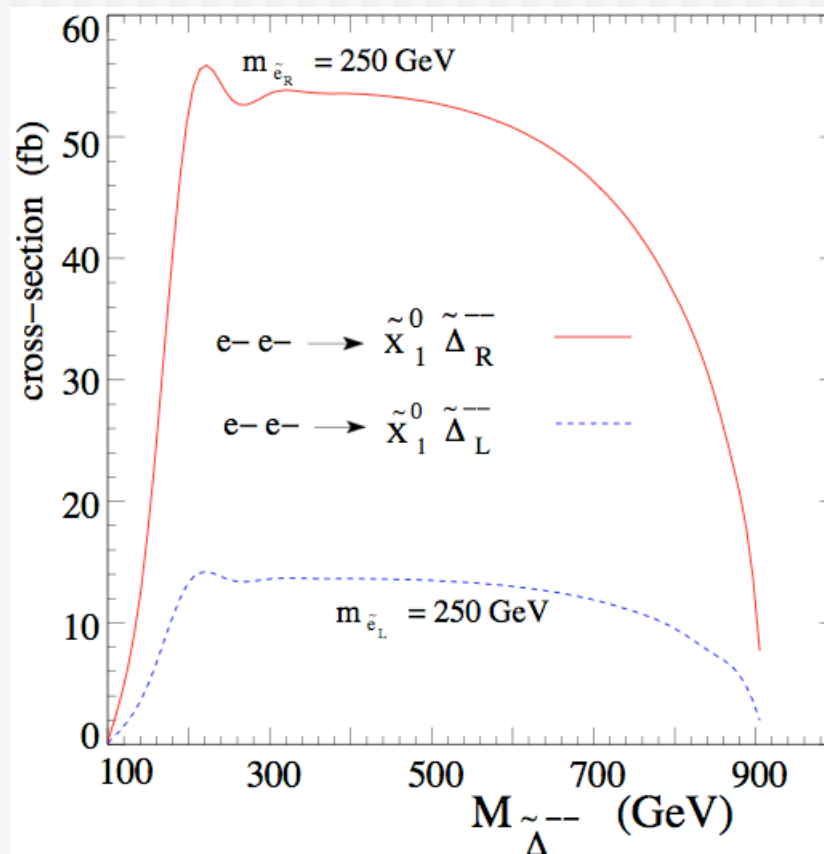
Sample point: **A**

*larger selectron mass
suppresses the production*

*production enhanced for
polarised beams*

*The input values for model
parameters also play a
significant role*

Production cross-section of the different chiral states



*polarised cross sections
for the two chiral states.*

Decays of the doubly charged Higgsinos

2-body decays

- $\tilde{\Delta}^{--} \longrightarrow \tilde{\ell}^- \ell^-$,
- $\tilde{\Delta}^{--} \longrightarrow \Delta^{--} \tilde{\chi}_i^0$,
- $\tilde{\Delta}^{--} \longrightarrow \tilde{\chi}_i^- \Delta^-$.

Assuming triplet Higgses to be heavier and degenerate in mass makes them kinematically inaccessible for relatively lighter doubly charged Higgsinos

• favored channel for decay which is $\tilde{\Delta}^{--} \longrightarrow \tilde{\ell}^- \ell^-$, provided $m_{\tilde{\ell}} < M_{\tilde{\Delta}^{--}}$.

or

$$\tilde{\Delta}^{--} \rightarrow \tilde{\ell}^{*-} \ell^- \rightarrow \ell^- \ell^- \tilde{\chi}_1^0.$$

Results

We focus on the 2-body (signal-1) and 3-body (signal-2) decay modes of the doubly charged Higgsino and look at the resulting signal events against the most dominant SM background.

We consider the following final states

$$(i) \quad e^-e^-E, \quad (ii) \quad \mu^-\mu^-E$$

We assume beam polarisation (-1,-1) for the left-chiral Δ

SM background:

$$e^- + e^- \rightarrow e^- + e^- + \bar{\nu}_l \nu_l$$

$$e^- + e^- \rightarrow \mu^- + \mu^- + \bar{\nu}_\mu \bar{\nu}_\mu + \nu_e \nu_e$$

		$\sqrt{s} = 500 \text{ GeV}$		
Cuts Used		SM	signal-1	signal-2
$E_e > 5 \text{ GeV}$	$ \eta_e < 3.0$	(-, -) 537.7 fb	(-, -) 123.8 fb	(-, -) 19.9 fb
$\cancel{E} > 10 \text{ GeV}$	$\Delta R_{ee} > 0.2$	(+, +) 15.1 fb	(+, +) 486.8 fb	(+, +) 78.1 fb
$E_e > 5 \text{ GeV}$	$ \eta_e < 1.5$	(-, -) 218.0 fb	(-, -) 102.7 fb	(-, -) 16.5 fb
$\cancel{E} > 100 \text{ GeV}$	$\Delta R_{ee} > 0.2$	(+, +) 3.8 fb	(+, +) 403.98 fb	(+, +) 65.1 fb
$E_e > 5 \text{ GeV}$	$ \eta_e < 3.0$	(-, -) 280.1 fb	(-, -) 123.8 fb	(-, -) 19.9 fb
$\cancel{E} > \sqrt{s}/2 \text{ GeV}$	$\Delta R_{ee} > 0.2$	(+, +) 3.3 fb	(+, +) 468.8 fb	(+, +) 78.1 fb
$E_e > 5 \text{ GeV}$	$ \eta_e < 1.5$	(-, -) 103.8 fb	(-, -) 102.7 fb	(-, -) 16.5 fb
$\cancel{E} > \sqrt{s}/2 \text{ GeV}$	$\Delta R_{ee} > 0.2$	(+, +) 0.103 fb	(+, +) 403.98 fb	(+, +) 65.1 fb
		$\sqrt{s} = 1 \text{ TeV}$		
$E_e > 5 \text{ GeV}$	$ \eta_e < 3.0$	(-, -) 1.13 pb	(-, -) 40.5 fb	(-, -) 14.0 fb
$\cancel{E} > 10 \text{ GeV}$	$\Delta R_{ee} > 0.2$	(+, +) 12.6 fb	(+, +) 156.4 fb	(+, +) 53.9 fb
$E_e > 5 \text{ GeV}$	$ \eta_e < 1.5$	(-, -) 238.9 fb	(-, -) 33.4 fb	(-, -) 11.7 fb
$\cancel{E} > 100 \text{ GeV}$	$\Delta R_{ee} > 0.2$	(+, +) 3.1 fb	(+, +) 129.2 fb	(+, +) 45.0 fb
$E_e > 5 \text{ GeV}$	$ \eta_e < 3.0$	(-, -) 605.9 fb	(-, -) 40.5 fb	(-, -) 14.0 fb
$\cancel{E} > \sqrt{s}/2 \text{ GeV}$	$\Delta R_{ee} > 0.2$	(+, +) 0.4 fb	(+, +) 156.4 fb	(+, +) 53.9 fb
$E_e > 5 \text{ GeV}$	$ \eta_e < 1.5$	(-, -) 106.0 fb	(-, -) 33.4 fb	(-, -) 11.7 fb
$\cancel{E} > \sqrt{s}/2 \text{ GeV}$	$\Delta R_{ee} > 0.2$	(+, +) 0.007 fb	(+, +) 129.2 fb	(+, +) 45.0 fb

Table 2: Signal and SM cross sections for the $e^-e^- \cancel{E}$ final states with different choice of kinematic cuts for both signal and background at the e^-e^- collider with center-of-mass energies $\sqrt{s} = 500 \text{ GeV}$ and $\sqrt{s} = 1 \text{ TeV}$. We also show the beam polarizations in parentheses. The ΔR is defined as $(\Delta R)^2 \equiv (\Delta\phi)^2 + (\Delta\eta)^2$ with $\Delta\eta$ and $\Delta\phi$ respectively denoting the separation in rapidity and azimuthal angle for the pair of particles under consideration.

We choose

$M_{\tilde{\Delta}_L^{--}} = 300$ GeV and $m_{\tilde{\ell}_{iL}} = 150$ GeV for *signal-1*, while for *signal-2*, $m_{\tilde{\ell}_{iL}} = 400$ GeV to study the signal at the $\sqrt{s} = 500$ GeV machine. The corresponding choice for the analysis at the $\sqrt{s} = 1$ TeV option is $M_{\tilde{\Delta}_L^{--}} = 500$ GeV, $m_{\tilde{\ell}_{iL}} = 250$ GeV for *signal-1*, while for *signal-2*, $m_{\tilde{\ell}_{iL}} = 550$ GeV.

Kinematic cuts are used which effectively suppress the SM background without losing out much on the signal events.

Kinematic distributions

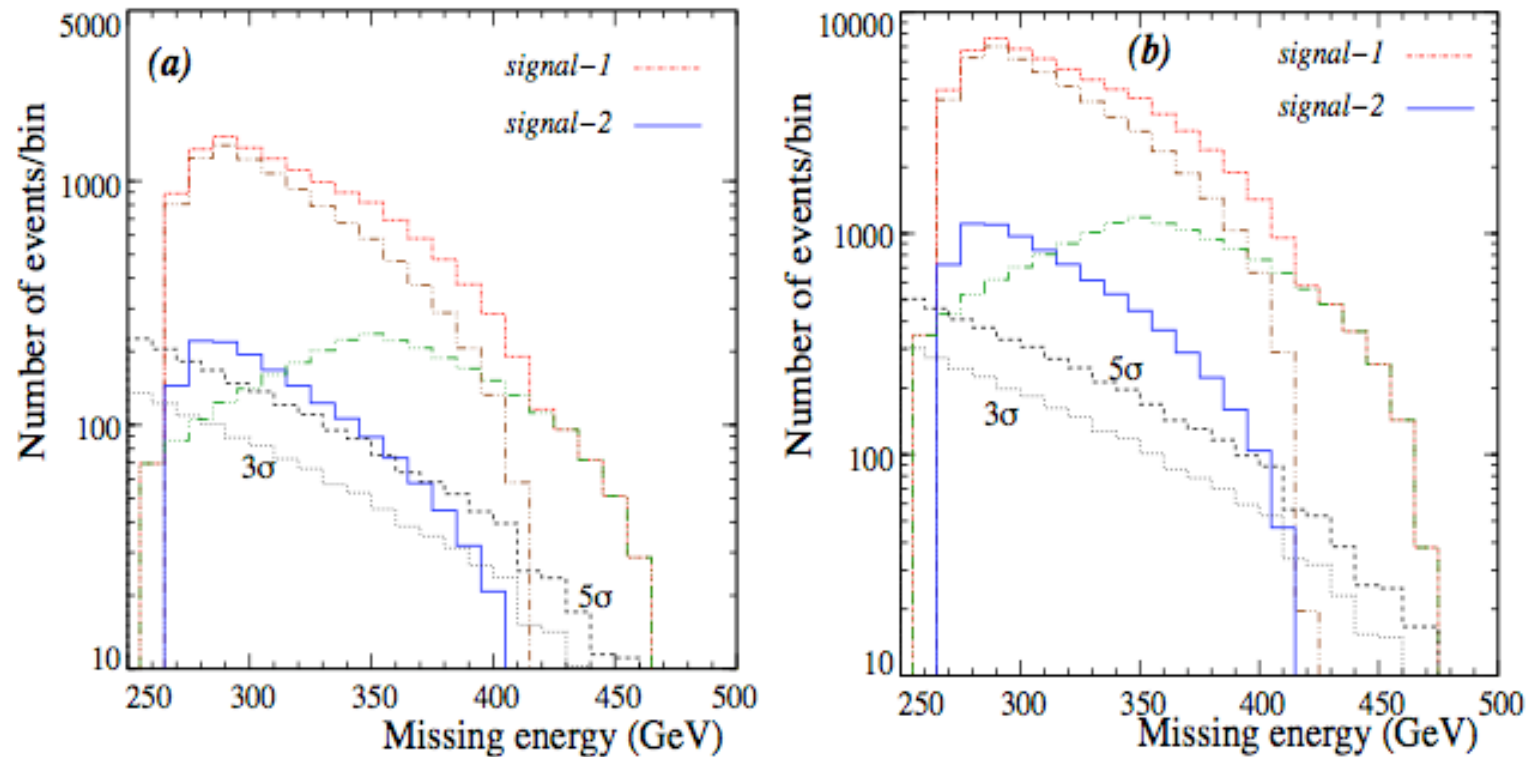


Figure 5: Binwise distribution of missing energy for both *signal-1* and *signal-2* for the final states e^-e^-E ($\sqrt{s} = 500 \text{ GeV}$). The broken ($-\cdots-$) brown lines correspond to the signal through $\tilde{\Delta}_L^-$ production while the broken ($-\cdots-$) green lines correspond to the signal events from \tilde{e}_L^- -pair production. Also shown in dashed and dotted dark lines are the 5σ and 3σ fluctuations in the SM background. Each binsize is 10 GeV. (a) $\mathcal{L} = 100 \text{ fb}^{-1}$, (b) $\mathcal{L} = 500 \text{ fb}^{-1}$.

$$M_{ee}^{edge} \approx \sqrt{M_{\tilde{\Delta}_L^{--}}^2 + M_{\tilde{\chi}_1^0}^2 - \sqrt{s}M_{\tilde{\chi}_1^0}}$$

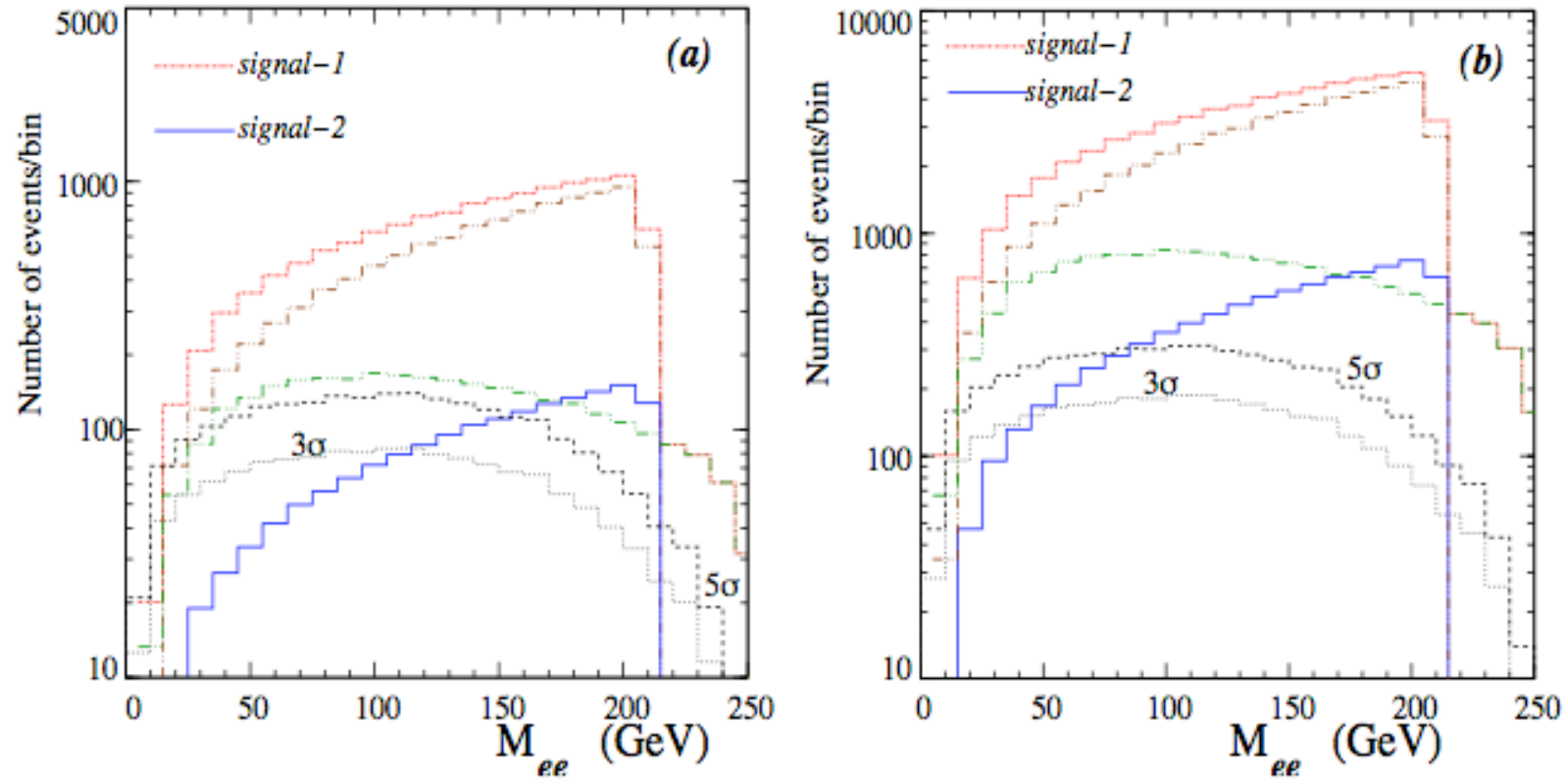


Figure 6: Binwise distribution of the invariant mass of the visible particles in the final state $e^- e^- \cancel{E}$ for both *signal-1* and *signal-2* ($\sqrt{s} = 500$ GeV). The broken $(-\cdot-\cdot-)$ brown lines correspond to the signal through $\tilde{\Delta}_L^{--}$ production while the broken $(-\cdot\cdot\cdot-)$ green lines correspond to the signal events from \tilde{e}_L^- -pair production. The background follows the notation of Fig 5. Each binsize is 10 GeV. (a) $\mathcal{L} = 100 fb^{-1}$, (b) $\mathcal{L} = 500 fb^{-1}$.

If one considers

$$|\Delta\eta| = |\eta_{e^-}^1 - \eta_{e^-}^2|$$

the signal peaks at $|\Delta\eta|=0$, while for the SM background it peaks beyond $|\Delta\eta|>1.2$

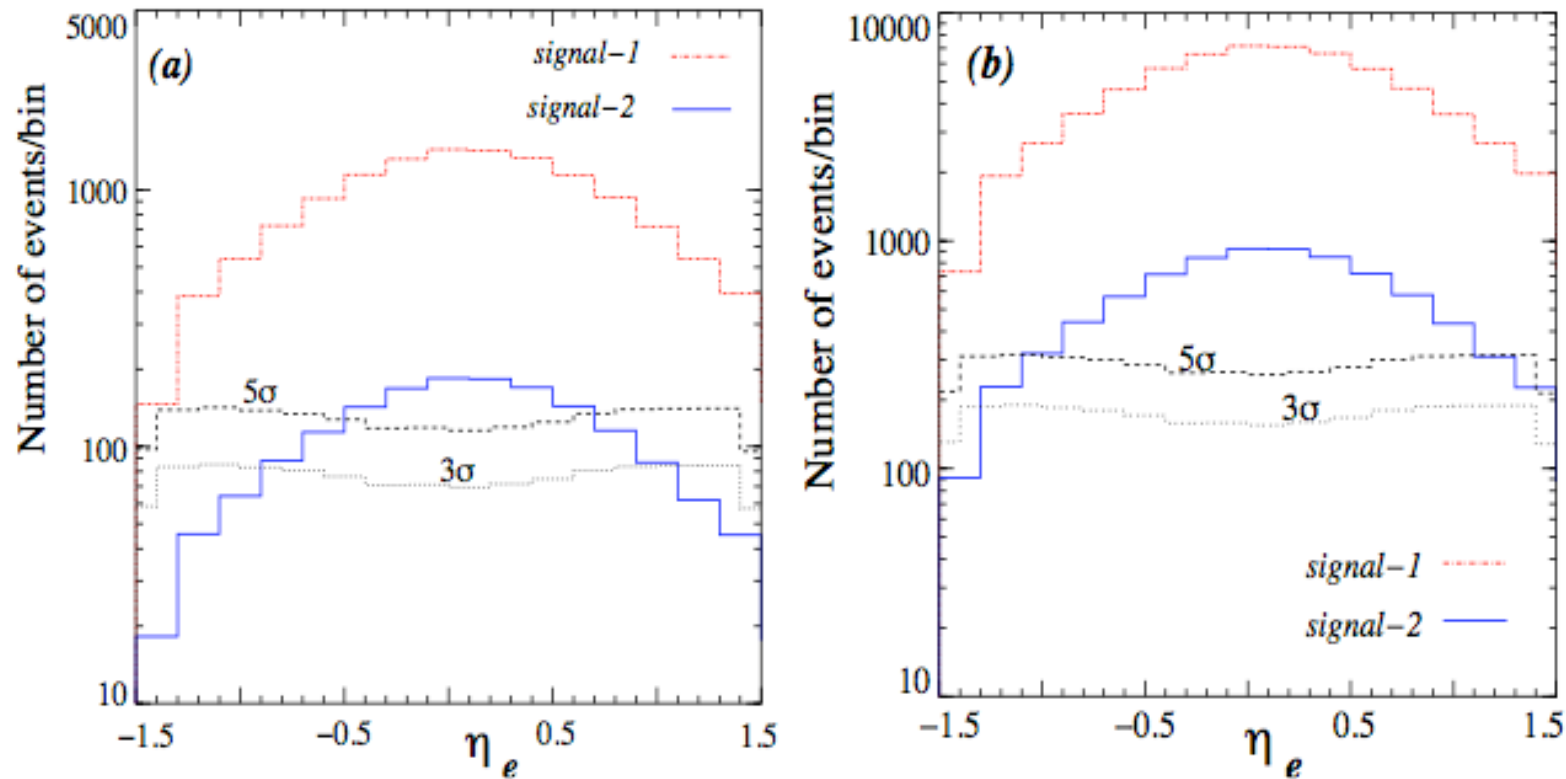


Figure 7: Binwise distribution of the rapidity of the e^- in the final state e^-e^-E for both *signal-1* and *signal-2* ($\sqrt{s} = 1 \text{ TeV}$). The background follows the notation of Fig 5. Each binsize is 0.2 radians. (a) $\mathcal{L} = 100 \text{ fb}^{-1}$, (b) $\mathcal{L} = 500 \text{ fb}^{-1}$.

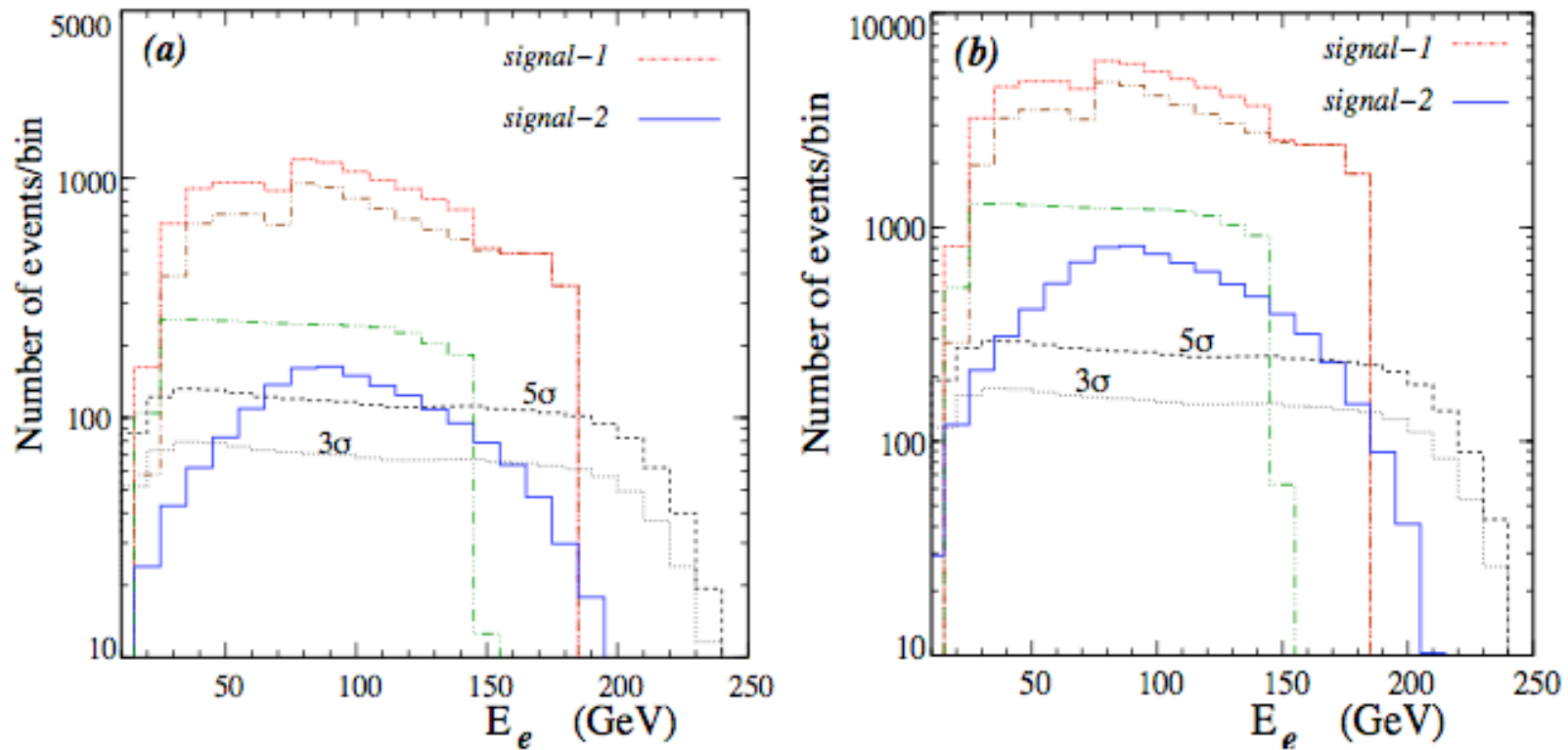


Figure 9: Binwise distribution of the energy of e^- in the final state $e^-e^-\cancel{E}$ for both *signal-1* and *signal-2* ($\sqrt{s} = 500$ GeV). The broken ($-\cdots-$) brown lines correspond to the signal through $\tilde{\Delta}_L^-$ production while the broken ($-\cdots-$) green lines correspond to the signal events from \tilde{e}_L^- -pair production. The background follows the notation of Fig 5. Each binsize is 10 GeV. (a) $\mathcal{L} = 100 \text{ fb}^{-1}$, (b) $\mathcal{L} = 500 \text{ fb}^{-1}$.

The right-handed higgsino $\tilde{\Delta}_R^{--}$

- ★ *Cross section enhanced for right-polarised electron beams.*
- ★ *SM background dominated by W-boson exchange is completely suppressed by this choice of beam polarisation*
- ★ *Signal is relatively background free.*
- ★ *Allows to probe much lower $\Delta L=2$ couplings.*

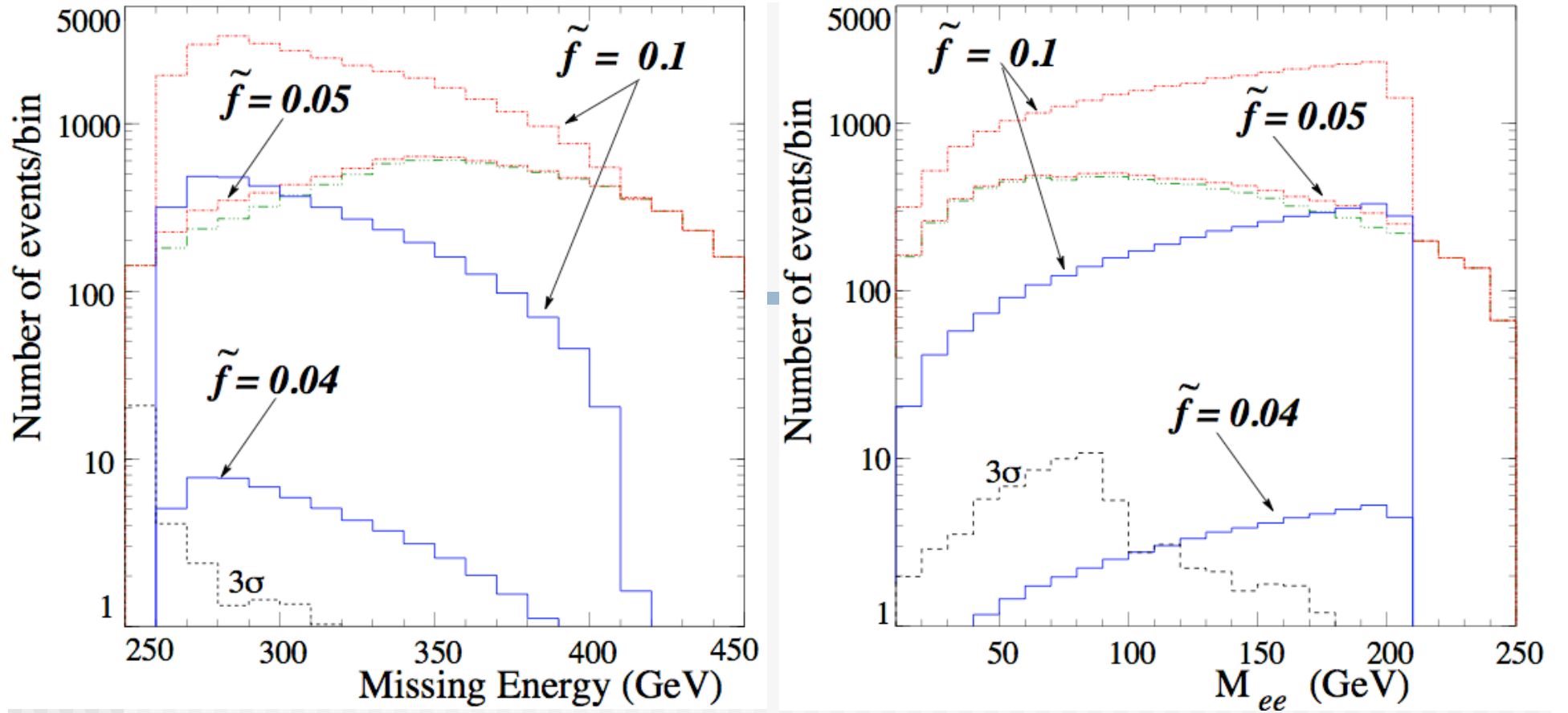


Figure 14: Binwise distribution of missing energy, invariant mass and energy of e^- for different values of the $\Delta L = 2$ coupling \tilde{f}_{ee} . The statistical fluctuations in the SM background is shown at 3σ in black (dashed) lines. Each binsize is 10 GeV while the luminosity is taken as $\mathcal{L} = 500 fb^{-1}$ (final state $e^-e^-\cancel{E}$). The green ($-\cdot-\cdot-$) line stands for the independent contribution from \tilde{e}_R^- -pair production for signal-1. Here $\sqrt{s} = 500$ GeV and $M_{\tilde{\Delta}_R^{--}} = 300$ GeV. For signal-1 shown in red lines, $m_{\tilde{e}_R} = 150$ GeV and for signal-2 shown in blue lines, $m_{\tilde{e}_R} = 400$ GeV.

Conclusions

- ★ *The presence of $\Delta L=2$ processes in theories beyond the SM can be probed directly at e^-e^- colliders*
- ★ *We show that production cross section for doubly charged Higgsinos in LRSUSY framework is large with polarised initial beams*
- ★ *The kinematic cuts can be effectively used to limit the SM background and give clear signal for LRSUSY*
- ★ *The beam polarisation proves an essential tool to distinguish the two chiral states giving the same final state*
- ★ *The doubly charged states can also become the NLSP which can result into quite spectacular signals.*
- ★ *We are presently studying the possible signatures for these exotics at hadron colliders.*